Low-Complexity Instantaneous GNSS Attitude Determination with Multiple Low-Cost Antennas

P.J.G. Teunissen[1,2], N. Nadarajah[1], G. Giorgi[3], P.J. Buist[2*]

[1] GNSS Research Centre, Curtin University of Technology, Australia
[2] DEOS, Delft University of Technology, The Netherlands
[3] Institute for Communications and Navigation, Technische Universität München
p.teunissen@curtin.edu.au

Biography

Peter Teunissen is professor of Geodesy and Earth Observation and Federation Fellow of the Australian Research Council. Nanthi Nadarajah is postdoc research fellow at the GNSS Research Centre of Curtin University, Perth, while Gabriele Giorgi and Peter Buist are both PhD candidates at the Mathematical Geodesy and Positioning (MGP) section of the Delft University of Technology. Their research is on GNSS attitude determination and satellite formation flying.

1 Abstract

Carrier phase integer ambiguity resolution is the key to fast and high-precision GNSS positioning and attitude determination. It is the process of resolving the unknown cycle ambiguities of the double-differenced carrier phase data as integers. Once this has been done successfully, the carrier phase data will act as very precise pseudo range data, thus making precise positioning and attitude determination possible. In this contribution, we describe and test the affine-constrained GNSS attitude model and compare its ambiguity resolution performance with that of MC-LAMBDA on a linear array of low-cost receiver/antennas.

2 Introduction

GNSS attitude ambiguity resolution is a rich field of current studies, with a wide variety of challenging (terrestrial, sea, air and space) applications. The earliest methods of attitude ambiguity resolution are the so-called motion-based methods. These methods take advantage of the change in receiver satellite geometry that is induced by the platform's motion. They are not applicable, however, on an epoch-by-epoch basis, as the presence of motion is needed per se. Another class of methods is the class of search-based methods. These methods are not necessarily dependent on motion and can therefore be used instantaneously in principle. They differ in the search domain used and in the objective function to be optimized.

More recent attitude determination methods search in the ambiguity domain. Several of them make use of the popular LAMBDA method, see e.g. [1, 2, 3, 4, 5, 6, 7, 8, 9, 10, 11, 12], as this method is known to be efficient and known to maximize the ambiguity success rate [13, 14, 15]. However, the standard LAMBDA method has been developed for unconstrained and linearly constrained GNSS models. The method is therefore not necessarily optimal for the GNSS attitude determination problem, for which often the multivariate antenna array geometry is provided as well. In order to do proper justice to this a priori information, the nonlinear constraints of the array geometry should be fully integrated into the ambiguity objective function. This is achieved by the recently developed multivariate constrained (MC-) LAMBDA method [16, 17, 18, 19]. But although this method has an increased success-rate performance in comparison with existing techniques, the complexity of its ambiguity search has increased as well. This is primarily due to the complexity of its search space which is not ellipsoidal anymore.

To avoid this complexity, we describe in this contribution an alternative to the MC-LAMBDA method. It is based on the affine-constrained GNSS attitude model as introduced in [20]. As it will be shown, the solution method's performance approaches that of the optimal multivariate constrained LAMBDA method, while its low complexity remains comparable with that of the unconstrained LAMBDA method. The results are demonstrated for a linear array of low-cost u-blox receiver/antennas.

3 GNSS Array Model: A Multivariate Formulation

In this section we introduce the GNSS model for a small-sized array of GNSS antennas. We make thereby use of the multivariate formulation as introduced in [21]. A frequent use is therefore made of the Kronecker product $\otimes$ and the vec-operator, see e.g., [22, 23].

The body of which the attitude needs to be determined

is assumed equipped with a body-fixed array of $r+1$ GNSS antennas all tracking the same $s+1$ satellites on the same f frequencies. Furthermore, we assume the array-size to be such that the differential atmospheric delays (troposphere and ionosphere) between the antennas can be neglected. With these assumptions, we can formulate the single-epoch, multi-frequency GNSS array model in *multivariate* form as

$$\mathrm{E}(Y) = MX + NZ \ , \ X \in \mathbb{R}^{3\times r} \ , \ Z \in \mathbb{Z}^{fs\times r} \qquad (1)$$

with $\mathrm{E}(.)$ the expectation operator, Y the $2fs \times r$ double differenced (DD) data matrix, (M, N) the $2fs \times (3+fs)$ design matrix, $X \in \mathbb{R}^{3\times r}$ the unknown real-valued baseline matrix and $Z \in \mathbb{Z}^{fs\times r}$ the unknown integer ambiguity matrix. The carrier phase and pseudo range data matrix is structured as $Y = [Y_\phi^T, Y_p^T]^T$, with $Y_\phi = [y_{\phi;1}, \ldots, y_{\phi;r}]$ and $Y_p = [y_{p;1}, \ldots, y_{p;r}]$, where $y_{\phi;\alpha} = [y_{\phi;\alpha,1}^T, \ldots, y_{\phi;\alpha,f}^T]^T$ and $y_{p;\alpha} = [y_{p;\alpha,1}^T, \ldots, y_{p;\alpha,f}^T]^T$ are the multi-frequency $fs \times 1$ vectors of DD phase and code observables of baseline α. For the entries of the design matrix (M, N), we have $M = (e_{2f} \otimes G)$ and $N = (L \otimes I_s)$, with e_{2f} the $2f \times 1$ vector of 1's, G the $s \times 3$ matrix of unit direction vectors that capture the DD relative receiver-satellite geometry and $2f \times f$ matrix $L = [\Lambda^T, 0^T]^T$, with $\Lambda = \mathrm{diag}(\lambda_1, \ldots, \lambda_f)$ the diagonal wavelength matrix, having the entries $\lambda_j = c/f_j$, $j = 1, \ldots, f$ (c is the speed of light; f_j is the jth frequency).

The dispersion of the GNSS array data matrix is assumed given by the $2fsr \times 2fsr$ variance matrix

$$\mathrm{D}(\mathrm{vec}(Y)) = Q_{YY} = P \otimes Q \qquad (2)$$

with $\mathrm{D}(.)$ the dispersion operator, $P = D_r^T D_r$ and $Q = \mathrm{blockdiag}(I_f \otimes Q_\phi, I_f \otimes Q_p)$, with Q_ϕ and Q_p the variance-matrices of the between-satellite single-differenced phase and code observables. The $r \times (r+1)$ differencing matrix D_r^T transforms between-satellite single-differenced observables into DD observables. For example, if the first antenna is taken as reference (master), then $D_r^T = [-e_r, I_r]$.

4 Three Different GNSS Attitude Models

In this section we briefly describe three different GNSS attitude models [17, 18, 19, 20, 21]. Let the dimension of the span of the r between-antenna baselines be $q \leq r$ and let the known baseline coordinates in the body-frame be collected in the $q \times r$ matrix B. Then $X = RB$, $R \in \mathbb{O}^{3\times q}$, in which $\mathbb{O}^{3\times q}$ denotes the set of $3 \times q$ matrices of which the q column vectors form an orthonormal span. The three attitude models differ in how use is made of the a priori given body-frame antenna-geometry in the relation $X = RB$. They are referred to as the *unconstrained* attitude model, the *affine-constrained* attitude model and the *orthonormality-constrained* attitude model.

4.1 The unconstrained attitude model

In this case, the relation $X = RB$ is not used in solving the multivariate array model (1). It is only used for computing the attitude matrix R. Thus first (1) is solved in a least-squares sense, after which the ambiguity resolved baseline matrix is used to determine the attitude matrix.

The multivariate LS-solution of (1) is given as

$$[\check{X}_{\mathrm{uc}}^T, \check{Z}_{\mathrm{uc}}^T]^T = \underset{X\in\mathbb{R}^{3\times r}, Z\in\mathbb{Z}^{fs\times r}}{\arg\min} ||\mathrm{vec}(Y - [M, N][X^T, Z^T]^T)||^2_{Q_{YY}} \qquad (3)$$

with $||.||^2_Q = (.)^T Q^{-1}(.)$. The suffix 'uc' is used to emphasize that this solution is not constrained by the body-frame antenna-geometry. Once the estimate $\check{X}_{\mathrm{uc}}$ is available, an estimate of the attitude-matrix R is determined in a LS-sense as

$$\check{R}_{\mathrm{uc}} = \arg \underset{R\in\mathbb{O}^{3\times q}}{\min} ||\mathrm{vec}(\check{X}_{\mathrm{uc}} - RB)||^2_{Q_{\check{X}_{\mathrm{uc}}\check{X}_{\mathrm{uc}}}} \qquad (4)$$

This nonlinear least-squares problem can be solved using one of the iterative descent methods, see e.g. [24].

4.2 The affine-constrained attitude model

The affine-constrained GNSS attitude model is defined in [20] as

$$\mathrm{E}(Y) = MX + NZ \ , \ XS = 0 \ , \ \mathrm{D}(\mathrm{vec}(Y)) = P \otimes Q \qquad (5)$$

with $X \in \mathbb{R}^{3\times r}$, $Z \in \mathbb{Z}^{fs\times r}$ and where S is an $r \times (r-q)$ basis matrix of the null space of B. This model is called *affine-constrained*, since the linear matrix constraint $XS = 0$ is equivalent to considering $X = RB$ as an affine transformation between body- and reference-frame, see [20].

The multivariate LS-solution of model (5) is given as

$$[\check{X}_{\mathrm{ac}}^T, \check{Z}_{\mathrm{ac}}^T]^T = \underset{X\in\mathbb{R}^{3\times r}, Z\in\mathbb{Z}^{fs\times r}, XS=0}{\arg\min} ||\mathrm{vec}(Y - [M, N][X^T, Z^T]^T)||^2_{Q_{YY}} \qquad (6)$$

Note that there are now two type of constraints involved. The linear constraints on the baseline matrix X ($XS = 0$) and the integer constraints on the ambiguity matrix Z ($Z \in \mathbb{Z}^{fs\times r}$). Although both type of constraints play an important role in strengthening the attitude model, the role they have to play is different. The primary purpose of the integer constraints is to be able to determine a precise attitude solution, while that of the linear constraints is to ensure that this can be done with sufficient probability of success.

Once the estimate $\check{X}_{\mathrm{ac}}$ of (6) is available, an estimate of the attitude-matrix R can be determined similar to (4), i.e. the role of $\check{X}_{\mathrm{uc}}, Q_{\check{X}_{\mathrm{uc}}\check{X}_{\mathrm{uc}}}$ is replaced by $\check{X}_{\mathrm{ac}}, Q_{\check{X}_{\mathrm{ac}}\check{X}_{\mathrm{ac}}}$.

4.3 The orthonormality-constrained attitude model

The orthonormality-constrained GNSS attitude model is defined in [21] as

$$\mathrm{E}(Y) = MX + NZ \ , X = RB \ , \ \mathrm{D}(\mathrm{vec}(Y)) = P \otimes Q \qquad (7)$$

with $X \in \mathbb{R}^{3\times r}$, $R \in \mathbb{O}^{3\times q}$ and $Z \in \mathbb{Z}^{fs\times r}$. Its multivariate LS-solution is given as

$$[\check{X}^T, \check{Z}^T]^T = \underset{X=RB, Z\in\mathbb{Z}^{fs\times r}, R\in\mathbb{O}^{3\times q}}{\arg\min} ||\mathrm{vec}(Y - [M,N][X^T, Z^T]^T)||^2_{Q_{YY}} \quad (8)$$

Again two type of constraints involved. But the linear constraints of (5) have now been replaced by the *nonlinear* orthonormality constraints of (7).

The above three attitude models, (1), (5) and (7), differ in the way they make use of the given body-frame antenna-geometry. Model (1) is the weakest as it does not use this information for solving X and Z. Model (7) is the strongest as it uses the full information provided by the relation $X = RB$.

4.4 Multivariate Integer Ambiguity Resolution

To show how the multivariate ambiguity objective functions of the three models compare, we make use of the following theorem.

Theorem (Multivariate orthogonal decomposition) Let $\hat{X}$, $\hat{Z}$ be the float solution of the array model (1) and let $\hat{E} = Y - M\hat{X} - N\hat{Z}$ be the corresponding matrix of LS-residuals. Furthermore, let $\hat{X}(Z) = (M^TQ^{-1}M)^{-1}M^TQ^{-1}[Y - NZ]$ and $X = RB$. Then the multivariate LS objective function can be orthogonally decomposed as,

$$||\mathrm{vec}(Y - MX - NZ)||^2_{Q_{YY}} = ||\mathrm{vec}(\hat{E})||^2_{Q_{YY}} + \left(||\mathrm{vec}(\hat{Z} - Z)||^2_{Q_{\hat{Z}\hat{Z}}} + ||\mathrm{vec}(\hat{X}(Z) - X)||^2_{Q_{\hat{X}(Z)\hat{X}(Z)}}\right) \quad (9)$$

with

$$||\mathrm{vec}(\hat{X}(Z) - X)||^2_{Q_{\hat{X}(Z)\hat{X}(Z)}} = ||\mathrm{vec}(\hat{X}(Z)P_S)||^2_{Q_{\hat{X}(Z)\hat{X}(Z)}} + ||\mathrm{vec}(\hat{X}(Z)P_S^\perp - RB)||^2_{Q_{\hat{X}(Z)\hat{X}(Z)}} \quad (10)$$

in which P_S and $P_S^\perp = I - P_S$ are the orthogonal projectors $P_S = S(S^TPS)^{-1}S^TP$ and $P_S^\perp = P^{-1}B^T(BP^{-1}B^T)^{-1}B$, respectively.

Proof The proof is given in [20].

When (9) and (10) are substituted into (3), (6) and (8), the three different ambiguity matrix ILS solutions $\check{Z}_{\mathrm{uc}}$, $\check{Z}_{\mathrm{ac}}$ and $\check{Z}$ follow. The unconstrained ILS ambiguity solution is given as

$$\check{Z}_{\mathrm{uc}} = \arg\min_{Z\in\mathbb{Z}^{fs\times r}} ||\mathrm{vec}(\hat{Z} - Z)||^2_{Q_{\hat{Z}\hat{Z}}} \quad (11)$$

while the affine-constrained ILS ambiguity solution reads

$$\check{Z}_{\mathrm{ac}} = \underset{Z\in\mathbb{Z}^{fs\times r}}{\arg\min} \left(||\mathrm{vec}(\hat{Z} - Z)||^2_{Q_{\hat{Z}\hat{Z}}} + ||\mathrm{vec}(\hat{X}(Z)P_S)||^2_{Q_{\hat{X}(Z)\hat{X}(Z)}}\right) \quad (12)$$

and the orthonormality-constrained ILS ambiguity solution is given as

$$\check{Z} = \underset{Z\in\mathbb{Z}^{fs\times r}}{\arg\min} \Big(||\mathrm{vec}(\hat{Z} - Z)||^2_{Q_{\hat{Z}\hat{Z}}} + ||\mathrm{vec}(\hat{X}(Z)P_S)||^2_{Q_{\hat{X}(Z)\hat{X}(Z)}} + ||\mathrm{vec}(\hat{X}(Z)P_S^\perp - \check{R}(Z)B)||^2_{Q_{\hat{X}(Z)\hat{X}(Z)}}\Big) \quad (13)$$

with $\check{R}(Z) = \underset{R\in\mathbb{O}^{3\times q}}{\arg\min} ||\mathrm{vec}(\hat{X}(Z)P_S^\perp - RB)||^2_{Q_{\hat{X}(Z)\hat{X}(Z)}}$.

Note that the ambiguity objective function of $\check{Z}_{\mathrm{uc}}$ is part of that of $\check{Z}_{\mathrm{ac}}$, while its ambiguity objective function is again part of that of $\check{Z}$. In the ambiguity objective function of $\check{Z}_{\mathrm{uc}}$ (cf. 11) only the distance of Z to $\hat{Z}$ is weighted, while in the ambiguity objective function of $\check{Z}_{\mathrm{ac}}$ (cf. 12) also the violation of the affine-constraint $XS = 0$ is weighted. It is this additional term which gives $\check{Z}_{\mathrm{ac}}$ a higher success-rate than $\check{Z}_{\mathrm{uc}}$.

Since the ambiguity objective functions of both $\check{Z}_{\mathrm{uc}}$ and $\check{Z}_{\mathrm{ac}}$ are quadratic forms in the entries of Z, both minimization problems (11) and (12) can be solved by means of the standard LAMBDA method. This is not the case with the ambiguity objective function of (13). Due to the nonlinear orthonormality constraint, the presence of the third term on the right-hand side of (13) makes this ambiguity objective function nonquadratic in Z. Hence, instead of the standard LAMBDA method, the multivariate-constrained (MC-) LAMBDA method needs to be applied to compute $\check{Z}$. The presence of the third term on the right-hand side of (13) gives $\check{Z}$ a higher success-rate than $\check{Z}_{\mathrm{ac}}$.

In the next section we will analyse the success-rate performances of $\check{Z}_{\mathrm{uc}}$, $\check{Z}_{\mathrm{ac}}$ and $\check{Z}$ for an array of multiple low-cost receiver/antennas.

5 The U-Blox Array Experiment

To test the three multivariate integer ambiguity estimators $\check{Z}_{\mathrm{uc}}$, $\check{Z}_{\mathrm{ac}}$ and $\check{Z}$, with low-cost antenna/receivers, an experiment with u-blox receivers was conducted at Curtin University, Perth, Australia, on 23 May 2011. Nine u-blox AEK-4T receivers were connected to nine ANN-MS-0-005 type patch antennas, which were mounted on a frame (Figure 1). As shown in Figure 2, antennas were placed symmetrically forming a planar array. Observations are collected for about two and a half hours with a 10 Hz sampling rate.

Fig. 1: The u-blox antenna frame.

The skyplot with elevation cut-off of 10° is shown in

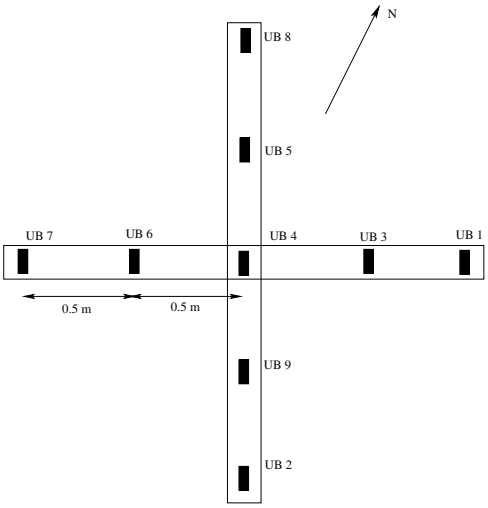

Fig. 2: The u-blox antenna geometry.

Figure 3, while Figure 4 shows the number of tracked satellites and their PDOP. We assumed the following elevation dependent model ([25]) for the standard deviation of the undifferenced single frequency L1 phase and code observables

$$\sigma_\theta = \sigma_0 \left(1 + a_0 \exp\left(\frac{-\theta}{\theta_0}\right)\right) \quad (14)$$

where θ is the elevation angle and $a_0 = 2$, $\theta_0 = 10°$, $\sigma_0 = 1.1$ m for the code observations and $\sigma_0 = 0.007$ m for the phase observations.

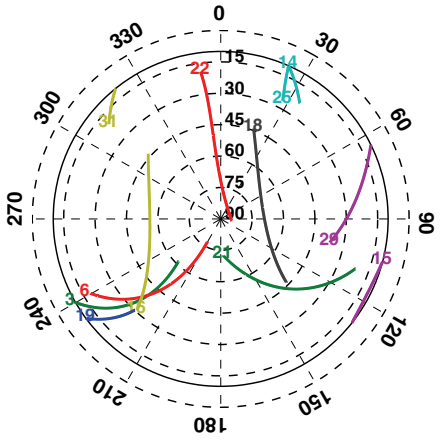

Fig. 3: Sky plot with 10° elevation cut-off.

5.1 The linear u-blox array

In this section we consider the performance of the linear u-blox array by analysing the spectra of conditional standard deviations, the ADOP, the success-rate and the linear array u-blox angular precision.

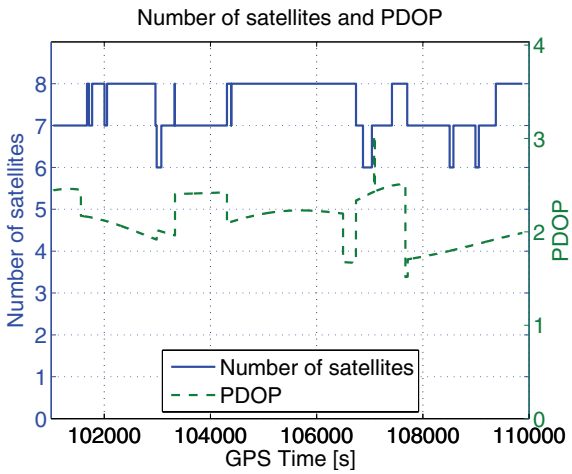

Fig. 4: Number of tracked satellites for 10° elevation cut-off and their PDOP.

5.1.1 On double-differenced and transformed spectra

To understand and illustrate the impact of the affine constraints, figures 5 and 6 show the linear array, unconstrained and affine-constrained, double-differenced (DD) and transformed spectra of conditional ambiguity standard deviations for a representative epoch and for varying number of baselines ($r = 1, 2, 3, 4$). Since 7 satellites are tracked in this case, there are $6 \times r$ single-frequency DD ambiguities.

In the unconstrained case, the DD-spectra all start at about 10 cycle, while for the affine-constrained case, they start at 10 cycle for $r = 1$, but then gradually start at lower values as the number of baselines, and therefore also the number of constraints, increases. This is due to the fact that the affine-constrained model gets stronger the more baselines are used. We also note, when comparing the unconstrained spectra (figure 5) with their affine-constrained counterparts (figure 6), that the affine-constrained DD-spectra only have one big discontinuity, while in the unconstrained case the number of discontinuities increases with the number of baselines. This is due to the fact that in the unconstrained case $3 \times r$ DD ambiguities need to be known before the remaining ambiguities can be determined with a high precision, while only 3×1 DD ambiguities are needed for the affine-constrained model. As a consequence of the fact that the affine-constrained spectra only have one discontinuity (from 3rd to 4th ambiguity), their transformed flat spectra will all be smaller than that of the unconstrained model. For $r = 4$, for instance, the transformed spectrum is at the level of 0.1-0.2 cycle, compared to the 0.8 cycle for the unconstrained case.

The *geometric mean* of the conditional ambiguity standard deviations is given by the ADOP (Ambiguity Dilution of Precision) [26, 27],

$$\text{ADOP} = \sqrt{|Q_{\hat{a}\hat{a}}|}^{\frac{1}{n}} \quad (15)$$

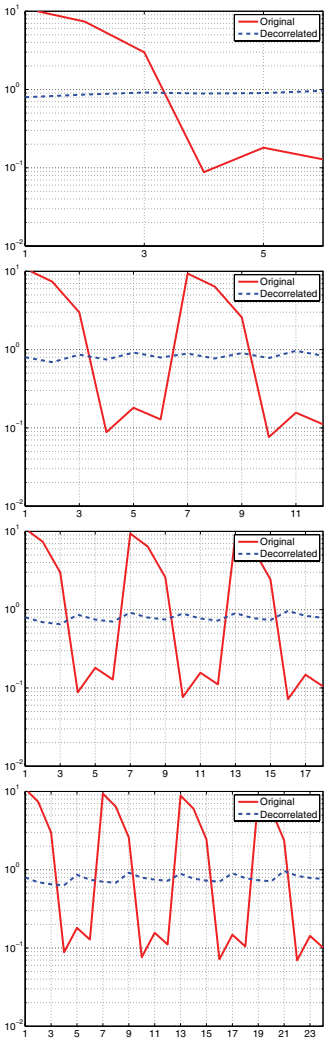

Fig. 5: Linear array, unconstrained spectrum of conditional standard deviations for $r = 1, 2, 3, 4$, from top to bottom. (red: double-differenced parametrization; blue: decorrelated parameterization).

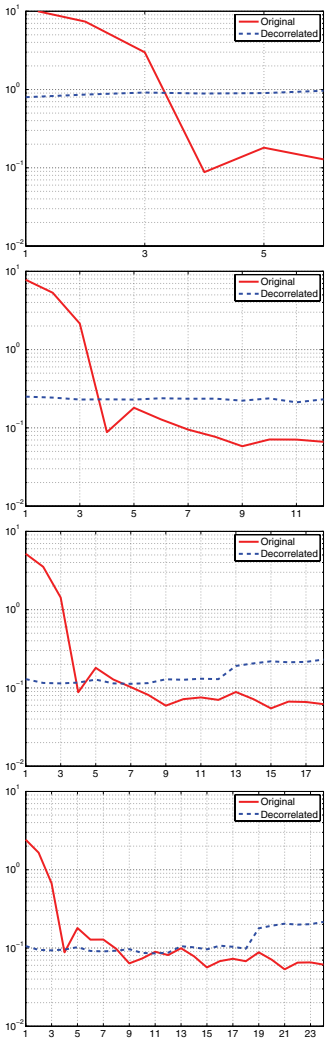

Fig. 6: Linear array affine-constrained spectrum of conditional standard deviations for $r = 1, 2, 3, 4$, from top to bottom (red: double-differenced parametrization; blue: decorrelated parameterization).

with $Q_{\hat{a}\hat{a}}$ the $n \times n$ ambiguity variance matrix. This easy-to-compute diagnostic measure has the advantage of being invariant for admissible integer ambgiuity transformations. Hence, it is a scalar diagnostic that measures the intrinsic precision of the ambiguities. The affine-constrained ADOP is shown in figure 7 as function of time. It shows the large reduction in ADOP-value when the affine-constraint gets into effect and then the gradual further decrease as the number of constraints increases.

5.1.2 The linear array success-rates

Table 1 shows the single-epoch u-blox linear array success rates for the three different constrained cases. As was already clear from the ADOP, one cannot have successful ambiguity resolution in the unconstrained case. In fact, due to the increase in ambiguity dimension, the unconstrained success-rates get smaller as more receivers are used. The

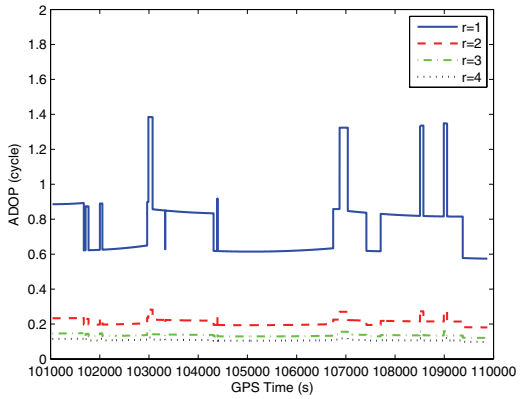

Fig. 7: The single-frequency, single-epoch, affine-constrained ADOP for $r = 1, 2, 3, 4$ as function of time.

MC-LAMBDA success-rates, on the other hand, are excellent. Already with three receivers the ambiguities of all

r	Receivers	LAMBDA		
		UC (%)	AC (%)	MC (%)
1	2-8	2.99	2.99	58.16
	1-7	4.43	4.43	87.14
2	2-8-5	0.36	89.57	100
	1-7-6	0.88	96.37	100
3	2-8-5-4	0.01	92.62	100
	1-7-6-4	0.13	96.74	100
4	2-8-5-4-9	0.00	93.41	100
	1-7-6-4-3	0.13	97.52	100

Table 1: Linear array, single-frequency, single-epoch, u-blox unconstrained (UC), affine-constrained (AC), and multivariate constrained (MC) ambiguity success rates (61601 samples)

r	Receivers	$\hat{\sigma}_H$ (^{o})	$\hat{\sigma}_E$ (^{o})	$\hat{\rho}_{HE}$
1	2-8	0.18	0.40	0.23
	1-7	0.16	0.49	-0.26
2	2-8-5	0.19	0.41	0.11
	1-7-6	0.16	0.43	-0.13
3	2-8-5-4	0.19	0.40	0.13
	1-7-6-4	0.15	0.41	-0.05
4	2-8-5-4-9	0.18	0.37	0.15
	1-7-6-4-3	0.14	0.34	-0.21

Table 2: Single-frequency, single-epoch, integer ambiguity resolved estimated angular precision (standard deviations and correlation coefficient) of u-blox linear array.

epochs are successfully resolved. The AC-LAMBDA results lie in between the unconstrained and fully-constrained results. Since the affine-constraints are only present for $r > q$, the results of AC-LAMBDA are of course equal to that of the unconstrained case for $r = 1$. However, the moment the affine-constraints come into play, we see a dramatic increase in the success-rates. Compare the single baseline case ($r = 1$), with the dual baseline ($r = 2$) case. And the success-rates increase with more baselines. Although one hundred per cent is not reached instantaneously, the results show that in the affine-constrained case only a few epochs would be needed to reach successful ambiguity resolution.

5.1.3 The linear array angular precision

The estimated standard deviations of heading and elevation (and their correlation) are shown in table 2. The single-epoch heading precision is better than 0.19 degrees and that of elevation is better than 0.49 degrees. The precision of elevation is poorer than that of heading, since with GNSS the height component is more poorly determined than the horizontal components.

6 Conclusions

In this contribution we described three different GNSS attitude models: the unconstrained model, the affine constrained and the multivariate nonlinear constrained model. The instantaneous ambiguity resolution performance of these three models was compared using data of low-cost receivers on a linear array. Although MC-LAMBDA has superior performance, it is shown that with only a few low-cost receiver/antennas also the low-complexity affine-constrained method can reach large single-frequency, single-epoch, success rates.

Acknowledgments

The first author is the recipient of an Australian Research Council Federation Fellowship (project number FF0883188). This support is gratefully acknowledged. Part of the presented work has been done in the context of the Australian Space Research Program GARADA project. We also thank our Curtin colleagues for assisting with the experiments.

References

[1] C Wang, R A Walker, and Y Feng. LAMBDA Method for Rigid Body Attitude Determination Based on GPS. *Acta Aeronautica et Astronautica Sinica*, 22(1):61–63, 2001.

[2] Furuno. Model SC-120: Satellite Compass. *http://www.furuno.co.jp/english/index.html*, 2003.

[3] D Lin, L Keck Voon, and N Nagarajan. Real-time Attitude Determination for Microsatellite by LAMBDA Method Combined with Kalman Filtering. *22nd AIAA International Communication Satellite Systems Conference, Monterey, US*, page 8, 2004.

[4] L Dai, K V Ling, and N Nagarajan. Real-time Attitude Determination for Microsatellite by LAMBDA Method Combined with Kalman Filtering. *Proceedings 22nd AIAA International Communications Satellite Systems Conference and Exhibit 2004 (ICSSC), Monterey, California, USA, 5p*, 2004.

[5] R Monikes, J Wendel, and G F Trommer. A Modified LAMBDA Method for Ambiguity Resolution in the Presence of Position Domain Constraints. *Proceedings of ION GPS-2005*, pages 81–87, 2005.

[6] L V Kuylen, F Boon, and A Simsky. Attitude Determination Methods Used in the PolarRx2@ Multi-antenna GPS Receiver. *Proceedings of ION GPS-2005, Long Beach, US*, page 11, 2005.

[7] M L Psiaki. Batch Algorithm for Global-Positioning-System Attitude Determination and Integer Ambiguity

Resolution. *Journal of Guidance, Control, and Dynamics*, 29(5):1071–1079, 2006.

[8] L V Kuylen, P Nemry, F Boon, A Simsky, and J F M Lorga. Comparison of Attitude Performance for Multi-Antenna Receivers. *European Journal of Navigation*, 4(2):1–9, 2006.

[9] A Hauschild and O Montenbruck. GPS Based Attitude Determination for Microsatellite. *Proceedings of ION GNSS, Forth Worth, TX, USA*, page 11, 2007.

[10] A Hauschild, G Grillmayer, O Montenbruck, M Markgraf, and P Vorsmann. GPS Based Attitude Determination for the Flying Laptop Satellite. *Small Satellites for Earth Observation, Springer Netherlands*, pages 211–220, 2008.

[11] J Pinchin. Enhanced Integer Bootstrapping for Single Frequency GPS Attitude Determination. *Proceedings of 21st ITM ION GPS*, pages 1290–1298, 2008.

[12] B Wang, L Miao, S Wang, and J Shen. A Constrained LAMBDA Method for GPS Attitude Determination. *GPS Solutions*, 13:97–107, 2009.

[13] P J G Teunissen. The Least-Squares Ambiguity Decorrelation Adjustment: a Method for Fast GPS Integer Ambiguity Estimation. *Journal of Geodesy*, 70:65–82, 1995.

[14] P J G Teunissen. An Optimality Property of the Integer Least-Squares Estimator. *Journal of Geodesy*, 73(11):587–593, 1999.

[15] S Verhagen and P J G Teunissen. New Global Navigation Satellite System Ambiguity Resolution Method Compared to Existing Approaches. *Journal of Guidance, Control, and Dynamics*, 29(4):981–991, 2006.

[16] P J G Teunissen. Integer Least Squares Theory for the GNSS Compass. *Journal of Geodesy*, (83):1–15, 2010.

[17] G Giorgi, P J G Teunissen, S Verhagen, and P J Buist. Testing a new multivariate GNSS carrier phase attitude determination method for remote sensing platforms. *J. Adv. Space Res.*, 46(2):118–129, 2010.

[18] G Giorgi, P J G Teunissen, S Verhagen, and P J Buist. Instantaneous Ambiguity Resolution in GNSS-based Attitude Determination Applications: the MC-LAMBDA Method. *Journal of Guidance, Control and Dynamics*, pages 1–12, 2011.

[19] P J G Teunissen, G Giorgi, and P J Buist. Testing of a New Single-Frequency GNSS Carrier Phase Attitude Determination Method: Land, Ship and Aircraft Experiments. *GPS Solutions*, 15(1):15–28, 2011.

[20] P J G Teunissen. The Affine Constrained GNSS Attitude Model and its Multivariate Integer Least-Squares Solution. *Journal of Geodesy, submitted*, pages 1–18, 2011.

[21] P J G Teunissen. A General Multivariate Formulation of the Multi-Antenna GNSS Attitude Determination Problem. *Artificial Satellites*, 42(2):97–111, 2007.

[22] D A Harville. *Matrix Algebra From A Statistician's Perspective*. Springer Verlag, New York, Berlin, Heidelberg, 1997.

[23] J R Magnus and H Neudecker. *Matrix Differential Calculus with Applications in Statistics and Econometrics*. John Wiley and Sons, 1995.

[24] P J G Teunissen. Nonlinear Least-Squares. *Manuscripta Geodaetica*, 15(3):137–150, 1990.

[25] H J Euler. On optimal filtering of GPS dual frequency observations without using orbit information. *Bulletin Geodesique*, 65:130–143, 1991.

[26] P J G Teunissen. A Canonical Theory for Short GPS Baselines. Part IV: Precision versus Reliability. *Journal of Geodesy*, 71(9):513–525, 1997.

[27] P J G Teunissen and D Odijk. Ambiguity Dilution of Precision: Definition, Properties and Application. *Proc. of ION GPS-1997, Kansas City MO*, pages 891–899, 1997.